Design Challenges Faced by Actively Stabilized High-Performance Aircraft

Timothy T. Takahashi[1]
Arizona State University, Tempe, AZ, 85287-6106

High performance aircraft tend to be slender with heavy components located along their fuselages. They also tend to feature swept wings and fins. On some aircraft, a center of gravity location may be specified so that the bare airframe longitudinal and lateral-directional frequencies are fast enough to avoid pilot (or autopilot) induced oscillations. On others, physical limitations may preclude sufficient static directional stability to ensure satisfactory unaugmented stability, i.e., hard limits on tail sizing or hard requirements on speed and altitude. This paper examines challenges the control law designer may face when the aerodynamic behavior of common control surfaces drives competing control laws which "fight" one another in an attempt to stabilize and control a high-performance aircraft.

Nomenclature

α	Angle-of-Attack (deg)
β	Sideslip Angle (deg)
AR	Wing Aspect Ratio (b / c)
b	Wing Reference Span
$\bar{c}$	Wing Reference Chord
CL	Lift Coefficient
Cm	Pitching Moment Coefficient
Cnβdynamic	Dutch-Roll Stability Parameter
dCl/dβ	Rolling Moment Coefficient per deg sideslip angle
dCn/dβ	Yawing Moment Coefficient per deg sideslip angle
dCY/dβ	Side-Force Coefficient per deg sideslip angle
Cmq	Pitch Dynamic Derivative
Clp	Roll Dynamic Derivative
Cnr	Yaw Dynamic Derivative
Ixx	Mass-Moment-of-Inertia in Roll (slug-ft^2)
Iyy	Mass-Moment-of-Inertia in Yaw (slug-ft^2)
Izz	Mass-Moment-of-Inertia in Pitch (slug-ft^2)
KEAS	Airspeed Knots Equivalent Airspeed
KTAS	Airspeed, Knots True Airspeed
LCDP	Lateral Control Departure Parameter (a metric of the impact of adverse yaw of the ailerons)
L/D	Aerodynamic Efficiency – Lift-to-Drag Ratio
M	Mach Number
n_Z	Load Factor (g's)
$\bar{q}$	Dynamic Pressure (lbf/ft^2)

I. Introduction

NOVEL AIRCRAFT CONFIGURATIONS present a broad challenge to the community. Because engineers have learned to understand issues associated with traditional tube-and-wing aircraft through a combination of theory, experiment, computation and service-experience, the strengths and weaknesses of these designs have been well documented. When engineers attempt to design unconventionally configured aircraft, particularly those capable of high-speed flight, there is much less publicly available information to rely upon. If engineers can solve structures, weight and propulsion challenges associated with high-speed flight, they must combine these mechanical elements into a holistic "vehicle" which demonstrates satisfactory stability and control across its intended flight envelope.

Classical flight dynamics models, as commonly used in industry, derive from a paradigm introduced at the dawn of the Twentieth Century. [1][2] As Bryan noted in 1904, "the main difficulty connected with the attempt to fly … is that of ... stability."[3] Bryan focused his initial work on the longitudinal stability problem because he incorrectly thought

[1] Professor of Practice (retired), School for Engineering of Matter, Transport & Energy, P.O. Box 876106, Tempe, AZ. Associate Fellow AIAA

© 2025 –TT Takahashi

that it was “not difficult to construct an aeroplane system which shall be transversely stable.”[2] Orville & Wilbur Wright would disagree; they empirically and experimentally devised a means to longitudinally, laterally and directionally stabilize and control their flying machine. [4] The Wright’s, in particular, found the lateral-directional problem more challenging than the longitudinal, as reflected in the Flyer’s complex wing-warping / rudder interconnect system. As Boyd notes, “the "practical men" were by and large nonplussed by [his] mathematics. Mathematicians just yawned.” [1]

Nonetheless, Bryan successfully demonstrated that the “stability of aeroplane systems can be made the subject of mathematical calculation.” [3] He modelled aircraft as if they were rigid bodies upon which gravitational and aerodynamic forces work. [3] He selected a body-fixed reference frame which translates in space as a function of time. [1] Six coupled equations of motion follow from there. Bryan also formalized the aerodynamic forces as a linear system following a Taylor-series expansion with partial derivatives of forces and moment with respect to various parameters. [3] As a mathematician, Bryan’s work did not focus on how one would determine these values but formalized how to mathematically show which combination of terms would lead to a system that would respond to disturbances in a way which would not excite any divergent nonlinearities. [3] Bryan was at the mercy of experimental data to feed his equations and lamented to the society that “until experiments are made … it will be impossible to solve the problem of stability.” [1][3]

In the intervening 121 years, little has changed; the controllability of a conceptual aircraft design cannot be assessed without an estimation of various linearized aerodynamic parameters.

II. Analytical Framework

In 1913, Bairstow, Jones & Thompson published a seminal report on aircraft stability. [5] Building upon the work of Byran, discussed above, they introduced a complete mathematical framework to analyze aircraft stability which is basically taught to this day. [6][7] They define stability in a manner “limited to small departures from the state of steady motion;” this is the essence of linearized analysis. At the same time, they believed that “all departures from the original state of motion may not be of equal importance;” therefore certain terms may be neglected. Yet they did realize that “rotary derivatives … are found to be of considerable importance." [5]

Bairstow’s nomenclature survives to this day, as it is an evolved version of Bryan’s original formulation. [5] The *x*-axis is aligned longitudinally; the *y*-axis laterally; the *z*-axis normal to a fixed body reference. They define angular velocities as *p*, *q* and *r* in a body fixed frame as functions of the flight path direction attitude (α=−θ), sideslip angle (β=−ψ) and bank angle (ϕ). More importantly, they define a convention where the equilibrium wind forces are nominally proportional to the weight of the aircraft and are independent of speed and size. They also define a convention where moment derivatives with respect to angular velocities are proportional to “weight,” the square of a reference length and inversely proportional to the square root of the forward velocity; in other words, a moment coefficient due to a “dimensionless angular velocity” rather than a physical one.

We note that Bairstow’s axis system (see FIGURE 1) while modelled on ship-building convention (frame stations grow increasing positive as one moves aft on the vehicle, water line heights grow increasingly positive as one moves up from the keel) does not conform to the modern “right-hand-rule.” Consequently, today’s sign convention used for flight dynamics has been inverted (see FIGURE 2) with the *x*-axis growing more positive as one moves forward, the *y*-axis aligned with a forward-facing pilot’s right hand, and the *z*-axis pointing downwards.

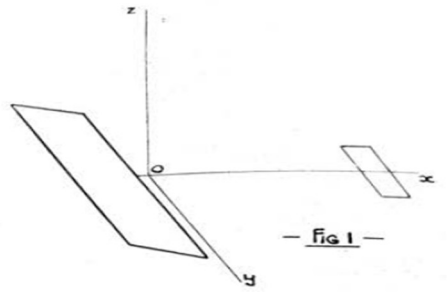

FIGURE 1 – The common axis system from Bairstow in 1913. [5]

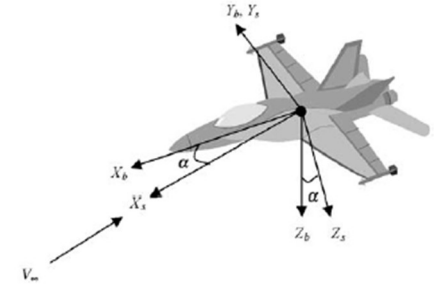

FIGURE 2 – Modern axis system – after Yechout. [7]

© 2025 –TT Takahashi

Today, dimensional forces and moments used to model static flight, are expressed as:

$$LIFT = C_L\ \bar{q}\ Sref \tag{1}$$
$$DRAG = C_D\ \bar{q}\ Sref \tag{2}$$
$$SIDEFORCE = C_Y\ \bar{q}\ Sref \tag{3}$$
$$PITCHINGMOMENT = C_m\ \bar{q}\ \bar{c}\ Sref \tag{4}$$
$$ROLLINGMOMENT = C_l\ \bar{q}\ b\ Sref \tag{5}$$
$$YAWINGMOMENT = Cn\ \bar{q}\ b\ Sref \tag{6}$$

Where *Sref* is the wing reference area, *b* is the wing reference span, $\bar{c}$ is the wing reference chord and $\bar{q}$ is the reference dynamic pressure.

Each of these coefficients is commonly expanded in a locally linearized Taylor series in terms of control surface deflections (δ) and sideslip angles (β). These are commonly presented as functions of speed (M) and attitude (α):

$$C_L \approx C_L(M,\alpha) + \frac{dC_L}{delev}(M,\alpha)\ \delta elev + \cdots \tag{7}$$
$$C_D \approx C_D(M,\alpha) + \frac{dC_D}{delev}(M,\alpha)\ \delta elev + \cdots \tag{8}$$
$$C_Y \approx \frac{dC_Y}{d\beta}(M,\alpha)\beta + \frac{dC_Y}{dail}(M,\alpha)\ \delta ail + \frac{dC_Y}{drud}(M,\alpha)\ \delta rud + \cdots \tag{9}$$
$$C_m \approx C_m(M,\alpha) + \frac{dC_m}{delev}(M,\alpha) + \cdots \tag{10}$$
$$C_l \approx \frac{dC_l}{d\beta}(M,\alpha)\beta + \frac{dC_l}{dail}(M,\alpha)\ \delta ail + \frac{dC_l}{drud}(M,\alpha)\ \delta rud + \cdots \tag{11}$$
$$C_n \approx \frac{dC_n}{d\beta}(M,\alpha)\beta + \frac{dC_n}{dail}(M,\alpha)\ \delta ail + \frac{dC_n}{drud}(M,\alpha)\ \delta rud + \cdots \tag{12}$$

Each of these locally defined coefficients (*CL, CD, Cm*) and derivatives (*dCn/dβ*, *dCl/drud*, …) can be measured in a wind tunnel, empirically estimated with a formula, or computed using some form of CFD code (either panel method or volume grid).

Today, dimensional moments used to model dynamic flight, are expressed in terms of the following common rate derivatives:

$$PITCHINGMOMENTDUETOPITCHRATE \approx \frac{1}{57.3}\left(C_{m_q}(M,\alpha)\ q + C_{m_{\dot{\alpha}}}(M,\alpha)\ \dot{\alpha}\right)\ \frac{\bar{q}\ \bar{c}^2\ Sref}{2\ VKTAS\ (\frac{6076}{3600})} \tag{13}$$
$$ROLLINGMOMENTDUETOROLLRATE \approx \frac{1}{57.3}\ C_{l_p}(M,\alpha)\ \frac{p\ \bar{q}\ b^2\ Sref}{2\ VKTAS\ (\frac{6076}{3600})} \tag{14}$$
$$ROLLINGMOMENTDUETOYAWRATE \approx \frac{1}{57.3}\ C_{l_r}(M,\alpha)\ \frac{r\ \bar{q}\ b^2\ Sref}{2\ VKTAS\ (\frac{6076}{3600})} \tag{15}$$
$$YAWINGMOMENTDUETOROLLRATE \approx \frac{1}{57.3}\ C_{n_p}(M,\alpha)\ \frac{p\ \bar{q}\ b^2\ Sref}{2\ VKTAS\ (\frac{6076}{3600})} \tag{16}$$
$$YAWINGMOMENTDUETOYAWRATE \approx \frac{1}{57.3}C_{n_r}(M,\alpha)\ \frac{r\ \bar{q}\ b^2\ Sref}{2\ VKTAS\ (\frac{6076}{3600})} \tag{17}$$

Physical pitch, roll and yaw rates, $\dot{\alpha}$, *q*, *p,* and *r*, are given in terms of units deg/sec. Speed is given in terms of knots true airspeed, *VKTAS*. Note that tradition has the "rotary derivatives" (*Cmq, Clp, Cnr*, …) given in terms of coefficients per dimensionless rates, rather than in terms of the rates themselves. The dimensional moments, in common nomenclatures, will be expressed in terms of lbf-ft.

It should be clear to the reader that even if the rotary derivatives are relatively invariant with Mach number, as a vehicle gains speed the moments developed due to a unit true angular velocity will decline.

© 2025 –TT Takahashi

III.Methods to Estimate the Aerodynamic Derivatives

Scale wind tunnel model testing has been the traditional basis for aerodynamic coefficient data used in flight dynamics models. The basic, steady coefficients arise from tests using model mounted at defined orientation (α,β) and subject to flow at a given Mach number. The unsteady coefficients (*Cmq*, *Clp*, *Cnr*, etc.) have proven more challenging to acquire. Beginning in the late 1940's, Bihrle devised a rotary balance fixture to measure the dynamic stability of proposed aircraft in a wind tunnel. [8] Above low speed work, the sort of testing proves challenging as the mounting apparatus can disrupt the flow due to its blockage, particularly at transonic and supersonic speeds.

Many texts use an "isolated component build-up" technique to estimate the "rotary derivatives." [6][7] For a simple, wing-body-tail configuration, a tractable engineering approximation may be made if one assumes that the pitch damping arises from the horizontal tail; all of the yaw damping arises from vertical fin, etc. From this paradigm, the dynamic derivatives may be estimated from algebraically complex functions of aircraft geometry, implied "downwash angles" and local lift-curve-slopes. The old USAF DATCOM method is a variation of this approach, where algebraically complex formulas are based on graphical "look up" of various parameters. [6][9]

A physics-based approach to estimate "rotary derivatives" is explained by Etkin and implemented in VORLAX. [6][10] Here, a steady state pitch, roll or yawing motion can be thought of in two ways: in the physical world, as a time-dependent Eulerian flow over a moving model OR in the computational world, as a quasi-static simulation of flow over a bent model. In the case of a pitching motion, q, the geometry is warped because by the time that the flow which first encounters the leading edge of a wing reaches the trailing edge, the aircraft has pitched up to an increased angle of attack; see FIGURE 3. This process may be repeated for a rolling motion (a corkscrew twist to the geometry) or for a yawing motion (a lateral camber to the geometry). The evergreen vortex-lattice-code, VORLAX, uses this approach to estimate pitch-rate, yaw-rate, and roll-rate dynamic derivatives. [10] Recent effort has been undertaken by Professor Takahashi and his collaborators to improve this code. [11]

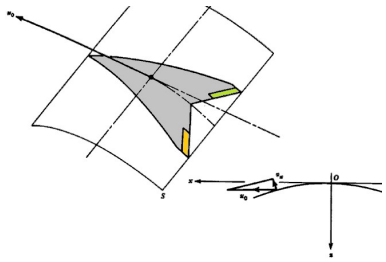

FIGURE 3 – Equivalent Cambered Model formulation from Etkin & Reid [6]

In recent years, considerable effort has been made to estimate these coefficients using unsteady CFD models. [12] While very computationally intensive, this approach has the ability to resolve if Bairstow's and Byran's implied linearization of moments about a dimensionless rate is appropriate. [5][2] Beyond our recent VORLAX work, authors such as Granata continue work on developing "medium fidelity methods" to estimate these derivatives. [13]

IV.Implications of the Dynamic Derivatives

While Bryan's linearized formulation provides great insight, we must recognize that aircraft control surfaces have only finite linearizable response and that deflected aerodynamic surfaces often exhibit considerable cross-coupling. Aircraft control surfaces are typically mechanically limited to +/- ~30º travel; while their actual response to deflection might not be precisely linear, an absence of "reversals," means that their effectiveness may be reasonably captured with the class linearized model. Cross coupling is an innate property of geometry. Consider side forces generated by a dorsal vertical fin and rudder at angle-of-attack; see FIGURE 4. As the aircraft pitches up or down, the centroid of the tail and rudder moment arm the height of the rudder (and vertical tail) moment arm falls or rises. In the wind axis, a "dorsal" vertical tail can easily become a "ventral" at high angles of attack. While its contribution to directional stability remains relatively constant with angle-of-attack, its contribution to dihedral effect will change sign (from increasing to decreasing the effective dihedral) given sufficient incidence. Similarly, the rolling

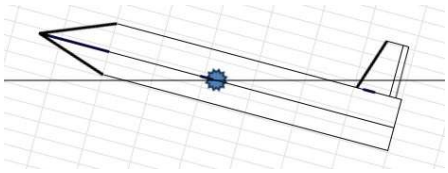

FIGURE 4 - Notional Aircraft at angle-of-attack.

© 2025 –TT Takahashi

moment due to rudder deflection will change in magnitude and sign with angle of attack. Since the aerodynamic forces on the body are driven by the oncoming wind, this has profound implications to the dynamic response of the airframe.

For many years, the United States military has defined compliance standards for aircraft stability and control. Since 1969, the standards define a precise "framework … which permits tailoring each requirement according to 1) the kind of airplane (class), 2) the job being done with the airplane (flight phase categories), and 3) how well the job must be done under various circumstances (levels)."[14] MIL 8785C from 1980 gives guidelines for desirable flying qualities often in terms of "equivalent-low-order-system" modal parameters, i.e., frequency and damping ratio, amenable to analysis using data available at the early design stages. [15] The later standard, MIL 1797 provides test cases and approaches to demonstrating compliance that often require high-fidelity simulations not suitable to preliminary design. [16] Both approximate closed-form and simulation-based approaches require a well-defined aerodynamic database.

MIL 8785C and MIL 1797 both recognize that ideal modal parameters for longitudinal short-period behavior must tailor the equivalent-low-order-system frequency, ω_{sp}, as a function of the pitch rate responsiveness of the aircraft, n_Z/α. [15][16] This criterion, known today as the "Control Anticipation Parameter" [17] represents the ratio of the instantaneous angular pitching acceleration generated per unit of steady state load factor.

$$CAP = \frac{\omega_{sp}^2}{\frac{n_Z}{\alpha}} \tag{18}$$

If the longitudinal short-period frequency is too slow, pilots have to "pump the controls" knowing that the aircraft will not respond to the input with any reasonable phase lag.

We may approximate the inherent short-period, rigid-body oscillatory mode of the aircraft at a given speed (M) and angle of attack (α) using a 1-DOF equivalent spring, mass, dashpot system; see FIGURE 5. [18] The short-period frequency is:

$$\omega_{sp} \approx \sqrt{\frac{-57.3\, C_{m_\alpha}\, \bar{q}\, S_{ref}\, \bar{c}}{Iyy}}, \tag{19}$$

while the pitch rate responsiveness may be estimated as:

$$\frac{n_Z}{\alpha} \approx \frac{57.3\, C_{L_\alpha}\, \bar{q}\, S_{ref}}{W}. \tag{20}$$

MIL 8785C also considers the need for an appropriate level of damping commensurate with the rigid body frequency. [15]

We may estimate the short-period damping ratio as:

$$\zeta_{sp} \approx -\frac{M_q + Z_\alpha/U_1}{2\,\omega_{sp}} \tag{21}$$

where the pitch angular acceleration due to pitch rate is:

$$M_q = C_{m_q} \frac{\bar{q}\, S_{ref} \bar{c}^2}{2\, Iyy\, VKTAS \left(\frac{6076}{3600}\right)} \tag{22}$$

and the normalized vertical acceleration due to angle of attack is:

$$\frac{Z_\alpha}{U_1} \approx -57.3\, C_{L_\alpha} \frac{\bar{q}\, S_{ref}}{\left(\frac{W}{g}\right) VKTAS \left(\frac{6076}{3600}\right)}. \tag{23}$$

and $VKTAS$ is the aircraft velocity in knots of true airspeed. [19]

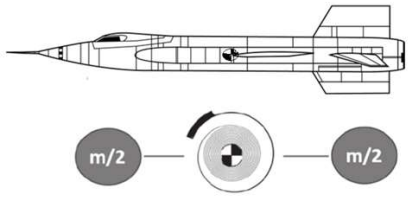

FIGURE 5 - Equivalent 1-DOF Spring Mass System for Short Period Analysis [15]

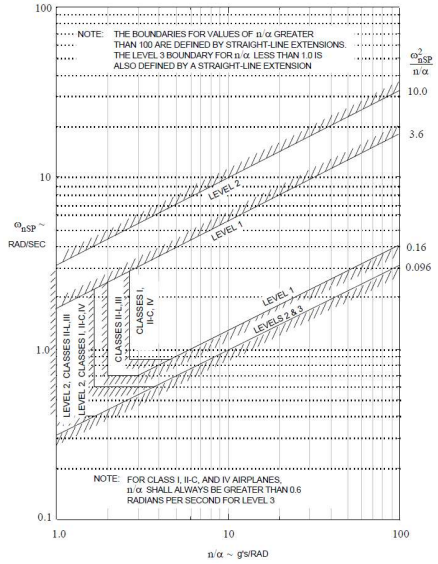

FIGURE 6 – MIL 8785C Control Anticipation Parameter chart for Takeoff & Landing. [12]

© 2025 –TT Takahashi

If the stick fixed longitudinal damping is inadequate, we may synthesize *Cmq* with a feedback gain. McRuer calls this the "equivalent stability derivative approach" to control law design. [20] Pitch damping is a function of the bare-airframe damping, *Cmq**, and a pitch rate dependent gain applied to the elevator:

$$C_{m_q}(M,\alpha) \approx C_{m_q}{}^{*}(M,\alpha) + \frac{dCm}{delev}\ 57.3\ K_{PITCHDAMP}\ \frac{q\ \bar{c}}{2\ VKTAS\left(\frac{6076}{3600}\right)} \tag{24}$$

The value of $K_{PITCHDAMP}$ is limited by the mechanical travel of the pitch control effector and the maximum anticipated pitch rate the control system is expected to encounter. With a total travel of +/- ~30º only a fraction of control power can be utilized by the stability augmentation controller; the remainder will be needed for basic static trim and/or pilot commands. Neither MIL 8785C nor MIL 1797A articulates specific pitch rate or percent control power to comply. Our understanding of production aircraft stability augmentation systems is that maximum pitch rates of +/- ~20º/sec and use of 25% of available control power are not unreasonable targets; this places an upper acceptable limit of a feedback gain to +/- ~0.35 º/(º/sec); see FIGURE 7.

MAXIMUM DEFL	ROTATIONAL RATE (º / sec)								
GAIN (º / º / sec)	1	2	3	4	5	10	20	30	40
0	0	0	0	0	0	0	0	0	0
0.01	0.01	0.02	0.03	0.04	0.05	0.1	0.2	0.3	0.4
0.02	0.02	0.04	0.06	0.08	0.1	0.2	0.4	0.6	0.8
0.03	0.03	0.06	0.09	0.12	0.15	0.3	0.6	0.9	1.2
0.04	0.04	0.08	0.12	0.16	0.2	0.4	0.8	1.2	1.6
0.05	0.05	0.1	0.15	0.2	0.25	0.5	1	1.5	2
0.1	0.1	0.2	0.3	0.4	0.5	1	2	3	4
0.2	0.2	0.4	0.6	0.8	1	2	4	6	8
0.3	0.3	0.6	0.9	1.2	1.5	3	6	9	12
0.4	0.4	0.8	1.2	1.6	2	4	8	12	16
0.5	0.5	1	1.5	2	2.5	5	10	15	20
1	1	2	3	4	5	10	20	30	40

FIGURE 7 – Commanded Control Deflections as a Function of Closed Loop Rate Gain and Sensed Rotational Rate.

MIL 8785C and MIL 1797 also provide guidelines for the preferred Dutch Roll frequency and damping. [14][15] The Dutch Roll frequency, in rad/sec, may be estimated by:

$$\omega_{dr} \approx \sqrt{\frac{57.3\ C_{n_{\beta dynamic}}\ \bar{q}\ S_{ref}\ b}{Izz}} \tag{25}$$

where: $C_{n_{\beta dynamic}} = \left(C_{n_\beta}\right)_{BODY} cos(\alpha) - \left(C_{l_\beta}\right)_{BODY} sin(\alpha)\left(\frac{Izz}{Ixx}\right)$. [18] (26)

Note that the values of directional stability ($dCn/d\beta$) and dihedral effect ($dCl/d\beta$) feeding this equation must be given in terms of body axis. So long as $C_{n_{\beta dynamic}}$ is positive, the aircraft will oscillate; if $C_{n_{\beta dynamic}}$ goes negative, the aircraft will depart.

The Dutch Roll expresses itself in terms of a mix of wing rocking (changes in ϕ) and tail wagging (oscillations in β). We may estimate the propensity to wing rock by the ϕ/β ratio: [7]

$$\phi/\beta \approx \left| \frac{\frac{dCl}{d\beta}}{\frac{dCn}{d\beta}} \frac{Izz}{Ixx}\ \frac{1}{\rho\ VKTAS\ (\frac{6076}{3600})} \right| \tag{27}$$

If $\phi/\beta >> 1$ the Dutch Roll expresses itself primarily as a wing rock; this makes a common "yaw damper" relatively ineffective. When faced with a high ϕ/β ratio airframe, the flight control team may select a feedback "roll damper" to damp the Dutch Roll mode. Since ϕ/β is dominated by the mass moment of inertia ratio (*Izz/Ixx*), body heavy aircraft tend to have such dynamics. As flight speeds increase, airframes tend to wing rock less. As altitudes increase (ρ decreases), airframes tend to wing rock more.

So long as $\phi/\beta << 10$ the Dutch Roll damping ratio may be estimated as:

$$\zeta_{dr} \approx -\frac{\left(N_r + \frac{Y_\beta}{U_1}\right)}{2\ \omega_{dr}} \tag{28}$$

© 2025 –TT Takahashi

where the normalized lateral acceleration due to sideslip is:

$$\frac{Y_\beta}{U_1} = 57.3\, C_{Y_\beta} \frac{\bar{q}\, S_{ref}}{(\frac{W}{g})\, VKTAS\, (\frac{6076}{3600})} \tag{29}$$

and the yaw angular acceleration due to yaw rate is:

$$N_r = C_{n_r} \frac{\bar{q}\, S_{ref}\, b^2}{2\, Izz\, VKTAS\, (\frac{6076}{3600})}. \tag{30}$$

Absent a directional "yaw damper," we may feed these equations with the bare airframe *Cnr**. If we contemplate a "yaw damper," both *Cnr* and *Clr* will be defined by a given feedback gain.

$$C_{l_r}(M,\alpha) \approx C_{l_r}{}^*(M,\alpha) + 2 \cdot 57.3 \frac{dCl}{drud}\, K_{YAWDAMP} \frac{VKTAS\, (\frac{6076}{3600})}{b} \tag{31}$$

$$C_{n_r}(M,\alpha) \approx C_{n_r}{}^*(M,\alpha) + 2 \cdot 57.3 \frac{dCn}{drud}\, K_{YAWDAMP} \frac{VKTAS\, (\frac{6076}{3600})}{b} \tag{32}$$

Where the gains, $K_{YAWDAMP}$, are given here in terms of engineering units, °rudder deflection per °/sec yaw rate.

The Roll-Mode is a first-order convergence/divergence seen as a tendency to damp roll rate when the aircraft executes a bank maneuver. The Roll-Mode is typically defined with the roll time constant, τ_R; this represents the time to achieve 63% of the peak roll rate based upon steady aileron input. We may estimate τ_R by:

$$\tau_R \approx -\frac{1}{L_p} \tag{31}$$

where:

$$L_p = C_{l_p} \frac{\bar{q}\, Sref\, b^2}{2\, Ixx\, VKTAS\, (\frac{6076}{3600})} \tag{32}$$

The Spiral-Mode is another first-order convergence/divergence that manifests itself as a tendency to roll into an ever-tightening spiraling turn (unstable) or roll out of a turn back to wings level flight (stable). [7] The unstable mode can lead to dangerous divergence. We may estimate τ_S by:

$$\tau_s \approx -\frac{1}{s} \tag{33}$$

where:

$$s \approx \frac{L_\beta N_r - N_\beta L_r}{L_\beta + N_\beta (\frac{I_{xz}}{I_{xx}})} \tag{34}$$

$$L_\beta = 57.3 \frac{dCl}{d\beta} \frac{q\, Sref\, b}{Ixx} \tag{35}$$

$$L_r = C_{l_r} \frac{\bar{q}\, Sref\, b^2}{2\, Ixx\, VKTAS\, (\frac{6076}{3600})} \tag{36}$$

$$N_\beta = 57.3 \frac{dCn}{d\beta} \frac{\bar{q}\, Sref\, b}{Izz} \tag{37}$$

When $s < 0$, the Spiral-Mode is stable. If $s > 0$, the Spiral-Mode is unstable. However, an aircraft can still have a satisfactory Spiral-Mode as long as this mode is not too unstable; $\tau_S < 4$-sec. [6]

When MIL 8785C directly requires aircraft response to roll commands to "not be oscillatory," it also implies that roll commands should not be divergent. Roll commands can excite the Short-Period or Dutch-Roll when the pilot executes a roll at a rate which excites these frequencies. [21] The critical roll rate, p_{crit}, can be found by searching for the lowest magnitude rate as predicted by the following equation:

© 2025 –TT Takahashi

$$p_{crit} \approx \pm 57.3 \min\left(\sqrt{\frac{57.3\frac{dCn}{d\beta}\bar{q}\,S\,b}{Iyy-I}}, \sqrt{\frac{-57.3\frac{dCm}{d\alpha}\bar{q}\,S\,\bar{c}}{Izz-Ixx}}\right). \quad (38)$$

If the aircraft rolls at this rate, energy from the commanded roll maneuver will excite either yawing and/or pitching motions. [22]

MIL 8785C requires attention to sideslip: "if roll or roll control excites sideslip, the flying qualities can be degraded by such motions as an oscillation of the nose on the horizon during a turn, by a lag or initial reversal in yaw rate during a turn entry, or by making it difficult for a pilot to quickly and precisely take up a given heading." [15]

We may estimate the equilibrium sideslip angle from a maximum uncoordinated aileron roll command to be:

$$\beta_{uncoordinated} \approx -\frac{\frac{dCn}{dail}\delta ail}{\frac{dCn}{d\beta}} \quad (39)$$

For LEVEL 1 flying qualities, MIL 8785C holds the maximum permissible sideslip to be adverse sideslip to be -6°> β>+2° during maneuvering flight and -10°> β>+3° during approach & landing; recall that a positive beta due to positive roll rate is "adverse." [15]

The Lateral Control Departure parameter was identified in the late 1950's after the Bell X-2 crash as a quasi-static metric which predicts whether the lateral control inputs stabilize or destabilize an airframe. [21] If adverse yaw due to rolling moment drives the aircraft to a sideslip, the sideslip may induce enough rolling moment to overcome the commanded moment, i.e., to have the response "reverse" after some lag.

Following Woodcock & Weissman, [23] We may estimate *LCDP* in two ways:

1. Bare-airframe, unaugmented: $LCDP = C_{n_\beta} - C_{l_\beta}\frac{(\frac{dC_n}{dail})}{(\frac{dC_l}{dail})}$ (40a)
2. Including aileron-rudder interconnect: $LCDP = C_{n_\beta} - C_{l_\beta}\frac{(\frac{dC_n}{dail}+\mathrm{K_{ARI}}\frac{dC_n}{drud})}{(\frac{dC_l}{dail}+\mathrm{K_{ARI}}\frac{dC_n}{drud})}$ (40b)

   If $LCDP > 0$, adverse yaw-due-to-roll is unlikely to lead to dynamic instability.
   If $LCDP < 0$, roll command inputs are likely to lead to a spin.

At this point we realize that there is one dynamic derivative which has gone unused, *Cnp*; the yawing moment due to dimensionless roll rate. In this paper, I introduce two novel screening parameters, the equilibrium sideslip angle due to roll rate:

$$\beta_{rollrate} \approx -\frac{C_{n_p}(M,\alpha)}{\frac{dCn}{d\beta}}\,\frac{p\,b}{2\;57.3\;VKTAS\,(\frac{6076}{3600})} \quad (41)$$

And its counterpart, rudder needed to oppose yawing moments due to roll rate:

$$\delta rud \approx \frac{C_{n_p}(M,\alpha)}{\frac{dCn}{drud}}\,\frac{p\,b}{2\;57.3\;VKTAS\,(\frac{6076}{3600})} \quad (42)$$

Absent a lateral "roll damper," we may feed these equations with the bare airframe *Clp** and *Cnp**. If we contemplate a "roll damper," both *Clp* and *Cnp* will be defined by a given feedback gain (either with or without aileron-rudder-interconnect ratio).

$$C_{l_p}(M,\alpha) \approx C_{l_p}{}^*(M,\alpha) + 2\cdot 57.3\left(\frac{dCl}{dail} + K_{ARI}\frac{dCl}{drud}\right)K_{ROLLDAMP}\frac{VKTAS\,(\frac{6076}{3600})}{b} \quad (43)$$

$$C_{n_p}(M,\alpha) \approx C_{n_p}{}^*(M,\alpha) + 2\cdot 57.3\left(\frac{dCn}{dail} + K_{ARI}\frac{dCn}{drud}\right)K_{ROLLDAMP}\frac{VKTAS\,(\frac{6076}{3600})}{b} \quad (44)$$

© 2025 –TT Takahashi

As with the longitudinal axis, the values of $K_{ROLLDAMP}$ and $K_{YAWDAMP}$ are limited by the mechanical travel of the various control effectors and the maximum anticipated rates the control system is expected to encounter. With a total travel of +/- ~30º only a fraction of control power can be utilized by the stability augmentation controller because MIL 8785C specifically states that up to 75% of available lateral-directional control power should be used when determining key cue speeds (like engine-inoperative minimum-control-speeds); thus only 25% of control power, in principle, is held in reserve for active stabilization.

MIL 8785C gives expected maximum bank angle change capability: LEVEL 1 capability for CLASS IV >~45º/sec for CATEGORY C approach & landing conditions. It also implies for precision flying and combat capability (CATEGORY A), CLASS IV aircraft should attain a peak roll rate >~90º/sec. Returning to FIGURE 7, we can see that the upper acceptable limit of feedback gain for roll damping under approach and landing is +/- ~0.20 º/(º/sec) and for precision flying is +/- ~0.10 º/(º/sec). [15]

Similarly, yaw damping systems should be able to damp yaw rates of up to +/- 50 º/sec. Returning to FIGURE 7, we can see that the upper acceptable limit of feedback gain for yaw damping is +/- ~0.2 º/(º/sec) in the absence of any commands arising through aileron-rudder-interconnect; lower otherwise.

V.Issues Noted Stabilizing Slender Airframes

This section documents both successful solutions and potential troublesome areas that arise when feedback control is used to improve the bare-airframe dynamics a high-speed airframes. In this paper, I only address airframes where the bare airframe is statically stable in the relevant axis.

A. Realistic Gains Can Provide Satisfactory Longitudinal Damping

In our first example, let us consider the X-15 on a representative mission: gliding flight at Mach 3 / ALT=60,000-ft with fuel tanks exhausted; see FIGURE 8. The aircraft weighs W=14,000-lbm. Reference dimensions are: $Sref$=197.5-ft^2; b=22.22-ft; $\bar{c}$=8.89-ft. Mass moment of inertia: Ixx=3600 slug-ft^2; Iyy=85,000 slug-ft^2; Izz=85,600 slug-ft^2; Ixz=-650 slug-ft^2. The relevant bare airframe aerodynamic properties are: $dCL/d\alpha$=0.0290, $dCm/d\alpha$=-0.173 1/º; Cmq^*= -7.03. Longitudinal control power from collective deflection of the all moving tailerons is: $dCm/delev$= -0.0104 1/º. [24]

Consider flight at 1980 KTAS;530 KEAS; $\bar{q}$ ~950 lbf/ft^2. From this, we estimate nZ/α ~ 22 g's/rad; ω_{SP} ~ 4.4 rad/sec (0.7 Hz). Thus, CAP ~ 0.87 which complies with LEVEL 1 standards for maneuvering, precision flight. However, the bare airframe aerodynamic damping proves ineffective at these flight conditions: ζ_{SP} ~ 0.04, which is far below LEVEL 3 minimums (ζ_{SP} > .15), LEVEL 2 minimums (ζ_{SP} > .25) and nowhere near the LEVEL 1 ideals (1.3 > ζ_{SP} > .35); see FIGURE 9a, overleaf. In order to achieve minimum LEVEL 1 damping, we need to employ a pitch rate feedback gain of at least 0.22º/(º/sec); this will synthesize Cmq ~ -105; see FIGURE 9b, overleaf. When faced with a pitch rate of +/- 20º/sec, the stability augmentation would command +/- 4.4º of collective elevator. This is a plausible gain which is unlikely to saturate the tailerons (which are used for pitch as well as lateral trim and stabilization).

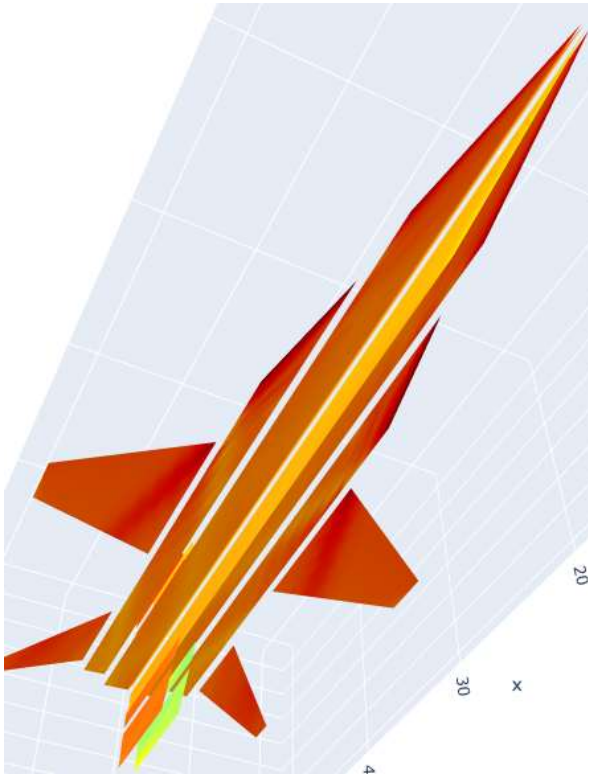

FIGURE 8 – North American X-15 VORLAX model used to estimate aerodynamics.

© 2025 –TT Takahashi

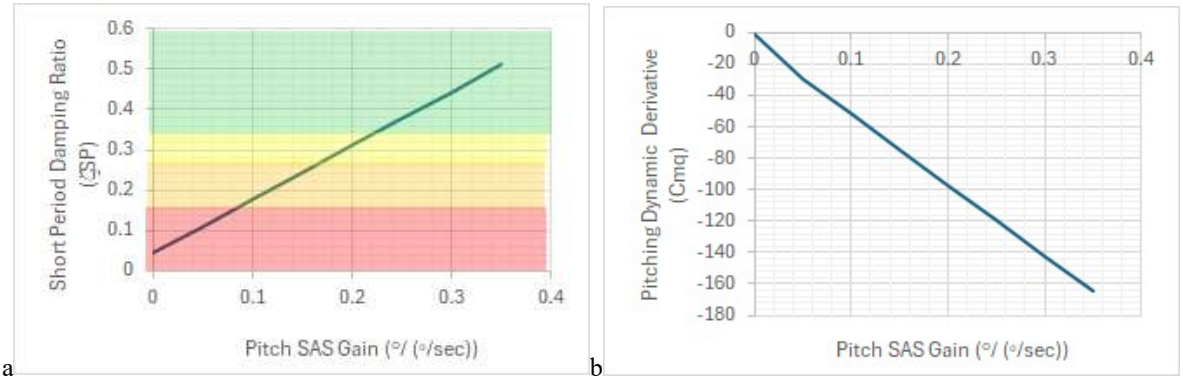

a b

FIGURE 9 – North American X-15 Mach 3 / ALT=60,000-ft / Empty Longitudinal Damping. a) Short Period Damping Ratio as a function of Pitch SAS gain. b) *Cmq* as a function of pitch SAS gain.

B. Unrealistic Gains Required to Achieve Satisfactory Longitudinal Damping

However, if we were to fly the X-15 at a higher altitude, for example ALT=100,000-ft, we would see a much less satisfactory trend. At 100,000-ft Mach=3 represents 1760 KTAS;208 KEAS; $\bar{q}$ ~147 lbf/ft^2. From this, we estimate $nZ/\alpha \sim 3.4$ g's/rad; $\omega_{SP} \sim 1.73$ rad/sec (0.28 Hz); thus, *CAP* complies with LEVEL 1 standards for precision flight. The bare airframe aerodynamic damping is even more ineffective at these flight conditions: $\zeta_{SP} \sim 0.02$; see FIGURE 10a. In order to achieve a minimum LEVEL 1 damping, we need to employ a pitch feedback gain of at least 0.65°/(°/sec); this will synthesize *Cmq* ~ -300; see FIGURE 10. When faced with a pitch rate of +/- 20°/sec, the stability augmentation would command +/- 13° of collective elevator. Given the quadruple use of the tailerons to provide pitch and lateral trim as well as pitch and roll stabilization, the stability augmentation system would likely saturate available control power. It should be no surprise that the X-15 employed a hydrazine reaction control system to augment aerodynamic control power when flown at such speeds and altitudes.

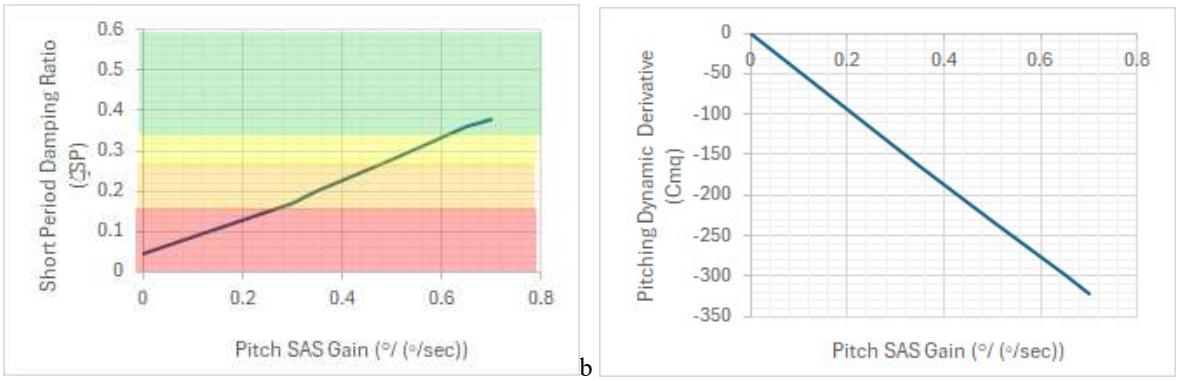

a b

FIGURE 10 – North American X-15 Mach 3 / ALT=100,000-ft / Empty Longitudinal Damping. a) Short Period Damping Ratio as a function of Pitch SAS gain. b) *Cmq* as a function of pitch SAS gain.

C. High Gains Needed to Provide Satisfactory Lateral Directional Damping at the Expense of Unstable Spiral Divergence

Let us return to the X-15 Rocket Plane in a 1-g glide at Mach 3 / ALT=60,000-ft with fuel tanks exhausted. We will now consider lateral-directional dynamics. The relevant bare airframe aerodynamic properties estimated using VORLAX are: $dCY/d\beta$=-0.0145 1/°, $dCl/d\beta$=-0.010 1/° and $dCn/d\beta$=+0.005 1/°. *Cnr**= -0.96; *Clp**= -0.21; *Clr**= -0.13 and *Cnp**= +0.00853. Lateral-Directional control power at this attitude is: *dCn/drud*= -0.022 1/°. *dCl/drud*= +0.001 1/°; the rudder provides strong control with modest adverse roll. The differential taileron provides: *dCl/dail*= -0.0008 1/°. *dCn/dail=+0.0002* 1/°; proverse yaw due to roll.

© 2025 –TT Takahashi

At the evaluated flight condition: 1980 KTAS;530 KEAS; $\bar{q}$ ~950 lbf/ft^2. From this, we estimate τ_{ROLL} =1.2-sec, which is satisfactory. We also estimate the Spiral Mode to be slightly unstable, marginally compliant with LEVEL 3 standards, τ_{SPRIAL}=~4-sec.

In terms of sideslip response, there is ample control power in both roll and yaw to trim more than 10^o sideslip. *LCDP* = +0.0048 with the rudder fixed, a favorable value. The strong directional stability keeps the equilibrium sideslip angle with full differential taileron and fixed rudder quite small; $\beta_{uncoordinated}$ = +/- 0.8^o.

Although the X-15 is body heavy (*Ixx* << *Iyy* and *Ixx* << *Izz*) the critical roll rate for inertia coupling exceeds 200 ^{o}/sec which is unexpected in flight.

It is the Dutch Roll mode that proves more troubling. *Cnβdynamic* = +0.0126; ω_{DR} ~ 5.9 rad/sec (0.94 Hz) which complies with LEVEL 1 standards for maneuvering, precision flight. Once again, we see that the bare airframe aerodynamic damping is ineffective: ζ_{DR} ~ 0.02, which is at the low end of LEVEL 2 (ζ_{DR} > .02) and nowhere near the LEVEL 1 ideals (ζ_{DR} > .19); see FIGURE 11a. In order to achieve minimum LEVEL 1 damping, we need to employ a yaw-rate feedback gain of at least 0.3^o/(^{o}/sec); this will synthesize *Cnr* ~ -12 with the unintended byproduct that it will drive *Clr* from -0.13 to +0.39; see FIGUREs 11b and 11c. Not only will the roll-due-to-yaw rate change sign with strong yaw damping, but the spiral mode will be further destabilized. With the extremely high gain needed to stabilize the Dutch Roll, the Spiral Mode time constant, τ_{spiral}, will decrease from a marginally acceptable 4-sec time-to-double to ~0.6-sec (see FIGURE 11d); such a short time constant demands excess pilot attention to compensate.

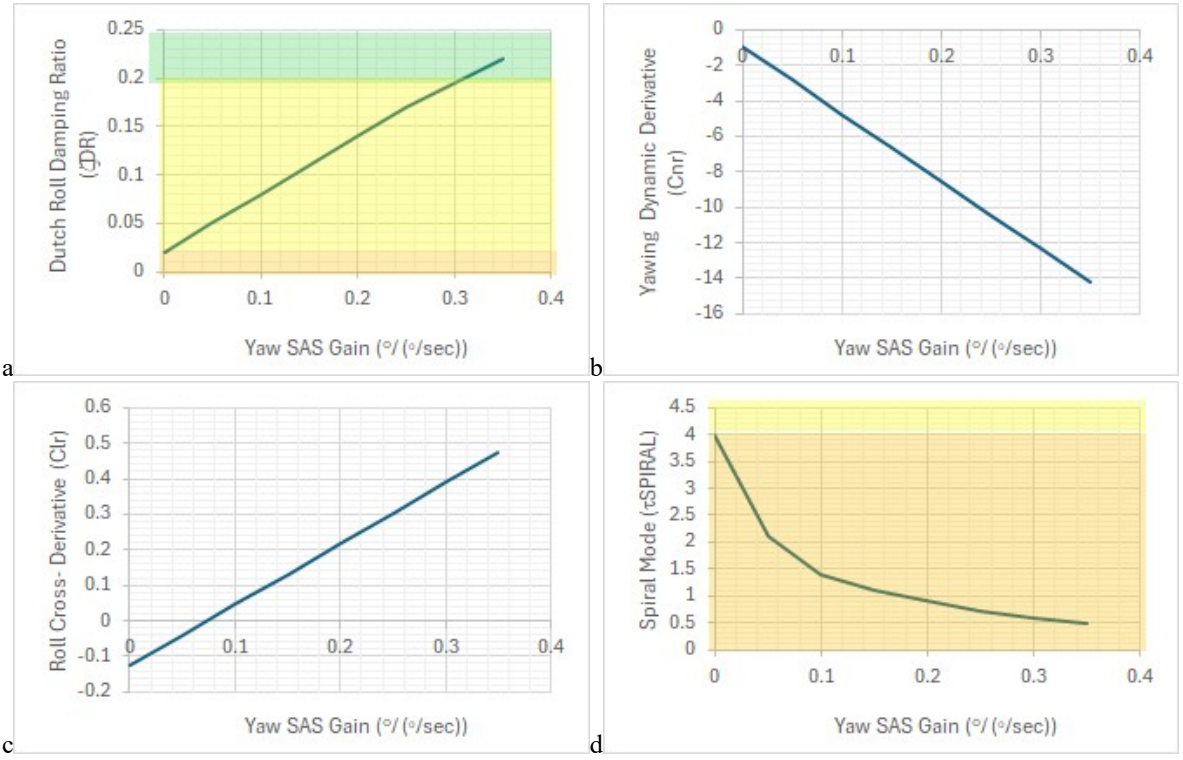

FIGURE 11 – North American X-15 Mach 3 / ALT=60,000-ft / Empty. a) Dutch Roll Damping Ratio as a function of Yaw SAS gain. b) *Cnr* as a function of yaw SAS gain, c) *Clr* as a function of yaw SAS gain, d) Spiral Instability as a Function of yaw SAS gain.

© 2025 –TT Takahashi

D. High Gains Needed to Provide Satisfactory Lateral Directional Damping Drive Roll Divergence at Low Speeds

In our next example, let us consider the Grumman F-14A Navy Fighter on final approach; see FIGURE 12. The wings are unswept to their minimum, Λ=22°. Flaps and slats are deployed. The aircraft weighs W=48,531-lbm. Reference dimensions are: $Sref$=564-ft^2; b=64.08-ft; $\bar{c}$=9.8-ft. Mass moment of inertia: Ixx=66,120 slug-ft^2; Iyy=265,681 slug-ft^2; Izz=327,689 slug-ft^2; Ixz=-2,537 slug-ft^2. [25]

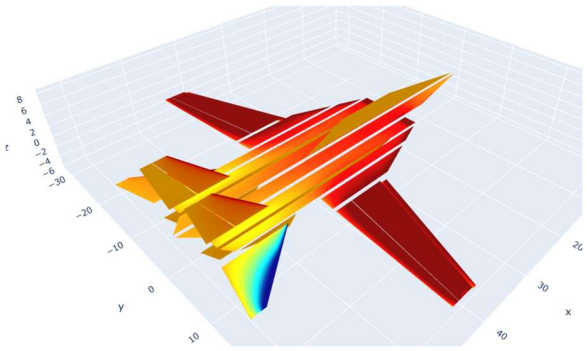

FIGURE 12 – F-14 Low Speed Configuration (Λ=22°) VORLAX model

We will consider its lateral-directional dynamics. Final approach is flown at α~6°. The relevant bare airframe aerodynamic properties estimated using VORLAX are: $dCY/d\beta$=-0.0140 1/°, $dCl/d\beta$=-0.017 1/° and $dCn/d\beta$=+0.0021 1/°. Cnr*= -0.23; Clp*= -0.40; Clr*= +0.33 and Cnp*= -0.055. Lateral-Directional control power at this attitude is: $dCn/drud$= -0.025 1/°. $dCl/drud$= -0.0001 1/°; the rudder provides strong control with minimal adverse roll. The differential taileron in conjunction with the spoileron provides: $dCl/dail$= -0.0024 1/°. $dCn/dail$=+0.0005 1/°; proverse yaw due to roll.

The F-14A flight control system lacked any form of aileron-rudder-interconnect. It featured yaw-rate feedback applied to its rudders; pitch-rate feedback applied to collective taileron, and roll-rate feedback applied to differential taileron / spoilerons.

For this work we evaluate the F-14A at a flight condition flown on final approach: 135 KTAS; 135 KEAS; $\bar{q}$ ~62 lbf/ft^2. From this, we estimate τ_{ROLL} =0.5-sec, which is satisfactory. We also estimate the Spiral Mode to be stable; fully compliant with LEVEL 1 standards.

In terms of sideslip response, there is ample control power in both roll and yaw to trim to more than 10° sideslip. $LCDP$ = +0.0030 with the rudder fixed, a favorable value. However, the modest static directional stability allows the equilibrium sideslip angle with full differential taileron and full spoileron with fixed rudder to grow quite large; $\beta_{uncoordinated}$ = +5.7° proverse – an objectionable value per MIL 8785C and MIL 1797A.

The critical roll rate for inertia coupling is quite slow: ~45°/sec. As this roll rate is below the minimums needed to comply with MIL 8785C LEVEL 1 guidelines, it seems probable that pilots will attempt to roll an F-14A at a rate which would excite inertia coupling.

As with the X-15, the Dutch Roll mode is the source of further troubles. $Cn\beta dynamic$ = +0.0029; ω_{DR} ~ 1.1 rad/sec (0.17 Hz) which just barely complies with LEVEL 1 standards for a Class IV aircraft flying an approach. The bare airframe aerodynamic damping is substandard: ζ_{DR} ~ 0.14, which is LEVEL 2 (ζ_{DR} > .02) and nowhere near the LEVEL 1 ideals ($\omega_{DR}\zeta_{DR}$ > .15); see FIGURE 13a. Moreover since $\frac{\phi}{\beta} \approx$ ~7, the Dutch Roll expresses itself primarily as a wing rock; this makes a common "yaw damper" relatively ineffective. In order to achieve minimum LEVEL 1 damping, we need to employ a yaw-rate feedback gain of at least 0.1°/(°/sec); this will synthesize Cnr ~ -0.34 with almost no change to Clr; see FIGUREs 13b and 13c.

We can also see that the F-14A, even without any roll SAS, exhibits a large amount of roll induced adverse sideslip (positive β from positive roll rate, p) because Cnp<0. We can see from FIGURE 14a that a modest 40°/sec roll rate will induce up to 2° adverse yaw which requires noticeable application of opposing rudder to balance. As the roll rates increase, the adverse yaw grows worse.

© 2025 –TT Takahashi

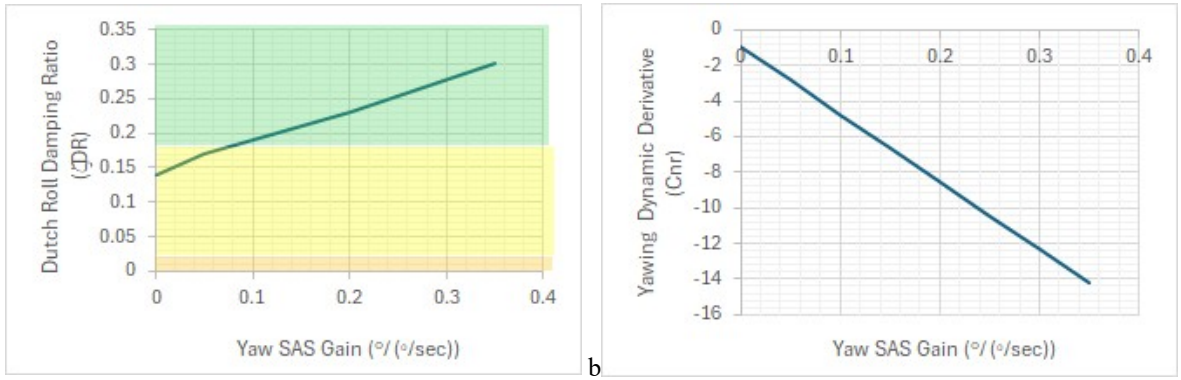

a b

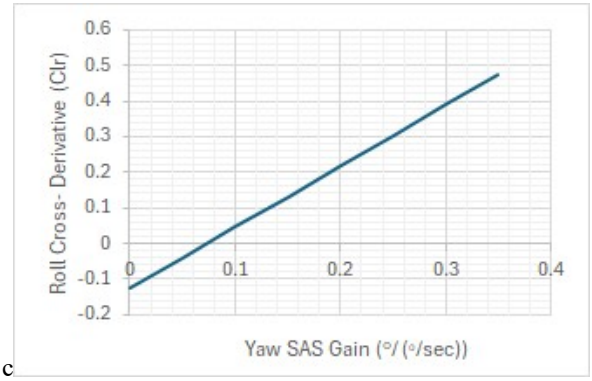

c

FIGURE 13 – Grumman F-14A Final Approach – Sea-Level/135 KEAS. a) Dutch Roll Damping Ratio as a function of Yaw SAS gain. b) *Cnr* as a function of yaw SAS gain, c) *Clr* as a function of yaw SAS gain

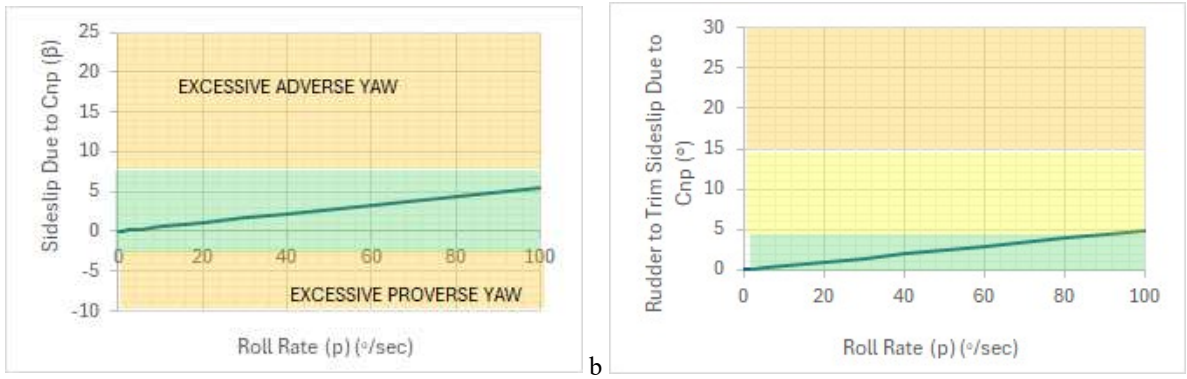

a b

FIGURE 14 – Grumman F-14A Final Approach – Sea-Level/135 KEAS. a) Sideslip due to *Cnp* as a function of roll rate, b) Rudder to trim sideslip due to *Cnp* as a function of roll rate. Roll SAS disengaged.

© 2025 –TT Takahashi

FIGURE 13 shows that there is no reasonable gain ($K_{YAWDAMPER}$ < 0.2 °/(°/sec)) that can drive the Dutch Roll damping to deadbeat (ζ>0.5). Thus, the Grumman engineers attempted to tackle the F-14A Dutch Roll mode suppression using a combination of Yaw and Roll dampers. The roll damper keys the differential taileron and spoileron position to sensed roll rate, p. It will impact the magnitude of the derivatives, *Clp* and *Cnp*. Because the "aileron" has proverse yaw, control laws which increase roll damping (making Clp more negative) will also drive *Cnp* more negative; a modest gain $K_{ROLLDAMPER}$ = -0.1 °/(°/sec) will nearly increase Clp from -0.4 to -1.1 with the side effect making *Cnp* much more negative; see FIGURE 15. Such a gain will induce crippling amounts of roll induced adverse sideslip; FIGURE 16a that a 40°/sec roll rate will induce more than 8° adverse yaw unless the pilot applies substantial coordinating rudder to balance. As the roll rates increase, the adverse yaw grows worse; high induced sideslip can easily stall the vertical fins or stall the engines and lead to a spin.

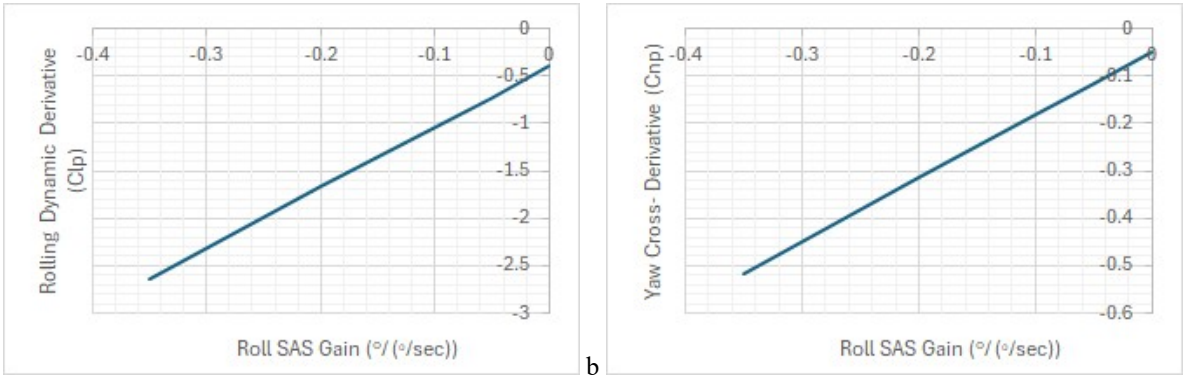

a b

FIGURE 15 – Grumman F-14A Final Approach – Sea-Level/135 KEAS. a) Roll Damping Derivative *Clp* as a function of Roll SAS gain. b) Yaw-to-Roll-Rate Cross Derivative *Cnp* as a function of Roll SAS gain.

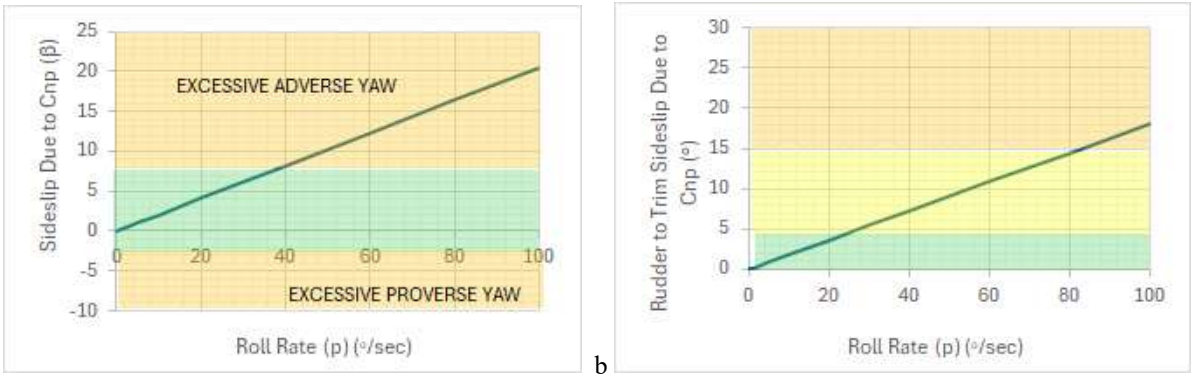

a b

FIGURE 16 – Grumman F-14A Final Approach – Sea-Level/135 KEAS. a) Sideslip due to *Cnp* as a function of roll rate, b) Rudder to trim sideslip due to *Cnp* as a function of roll rate. Roll SAS gain -0.1 °/(°/sec).

© 2025 –TT Takahashi

E. Excessive Gains Needed to Provide Satisfactory Lateral Directional Damping and Roll Responsiveness Also Drive Dangerous Amounts of Adverse Yaw at Supersonic Speeds

In our final example, let us consider the Bell X-2 rocket plane. [26] In reality, it was dangerous to fly; the X-2 had inadequate static directional stability, excessive adverse yaw from its ailerons, an intentionally disabled rudder (locked out at supersonic speeds), poor Dutch Roll **and** Short Period damping along with a tendency to inertia couple. [27] In previous work, we demonstrated that its open-loop flying characteristics would markedly improve with a substantially larger vertical fin. [27] For this paper, we examine if a combined roll and yaw damper closed-loop control could render its Dutch Roll, Spiral and Roll characteristics satisfactory without further aerodynamic modifications and if so, what would its gains have to be?

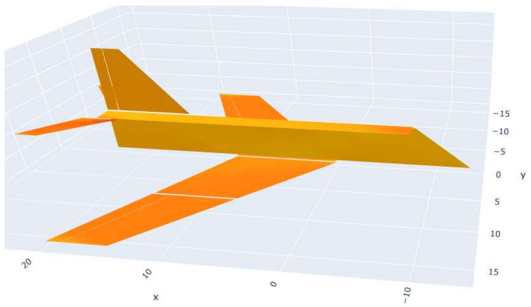

FIGURE 17 – Bell X-2 VORLAX model

As it nears fuel exhaustion at high speeds and altitudes, the X-2 weighs W=12,375-lbm. [21][28] Reference dimensions are: $Sref$=258-ft^2; b=32.17-ft; $\bar{c}$=8.32-ft. [28] Mass moment of inertia: Ixx=5,043 slug-ft^2; Iyy=25,474 slug-ft^2; Izz=29,106 slug-ft^2; Ixz=782 slug-ft^2. [21]

For this analysis, we will consider the X-2's combined longitudinal and lateral-directional dynamics nearing fuel exhaustion at high speeds and high altitudes. At Mach 3.2 and ALT=70,000-ft, which is flight at 1850 KTAS; 445 KEAS; $\bar{q}$ ~ 672 lbf/ft^2. This represents nZ=1 flight when flown at α~3º. The relevant bare airframe aerodynamic properties estimated using VORLAX at this speed at attitude is: CL=0.07; $dCL/d\alpha$ = +0.025 1/º; $dCm/d\alpha$ =-0.048 1/º; $dCY/d\beta$=-0.012 1/º, $dCl/d\beta$=-0.015 1/º and $dCn/d\beta$=+0.0004 1/º. Cmq*= *-0.3; Cnr*= -0.16; Clp*= -0.20; Clr*= +0.05 and Cnp*= +0.031. Longitudinal control power at this speed is: $dCm/delev$ = -0.0048 1/º. Lateral-Directional control power at this speed and attitude is: $dCn/drud$= -0.0003 1/º. $dCl/drud$= +0.00015 1/º; the rudder provides weak control with adverse roll. The wing mounted ailerons provide: $dCl/dail$= 0.0008 1/º. $dCn/dail$=-0.0002 1/º; strong adverse yaw due to roll in light of its body heavy mass properties and weak static directional stability. [28]

From this, we estimate the longitudinal dynamic response as follows: nZ/α ~ 20.1 g's/rad; ω_{SP} ~ 1.33 rad/sec (0.21 Hz); thus CAP = ~0.09. CAP falls well below LEVEL 1 standards for precision flight but is barely LEVEL 1 for general Phase B operations. The bare airframe aerodynamic damping is ineffective at these flight conditions: ζ_{SP} ~ 0.08; see FIGURE 18a. In order to achieve a minimum LEVEL 1 damping, we need to employ a pitch feedback gain of at least 0.35º/(º/sec); this will synthesize Cmq ~ -60; see FIGURE 18b. When faced with a pitch rate of +/- 20º/sec, the stability augmentation would command +/- 7º of elevator. This level of feedback is high, but reasonable provided that the pilot does not utilize substantial elevator for trim.

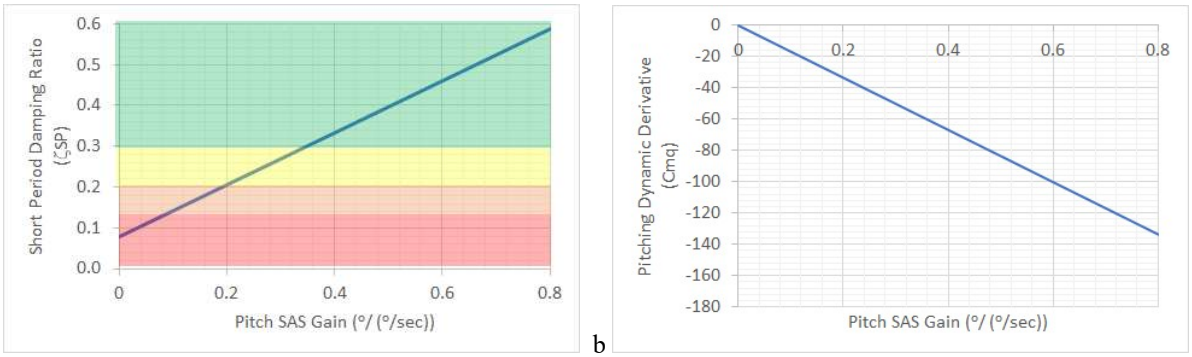

FIGURE 18 – Bell X-2 Mach 3.2 / ALT= 70,000-ft / Empty Longitudinal Damping. a) Short Period Damping Ratio as a function of Pitch SAS gain. b) *Cmq* as a function of pitch SAS gain.

© 2025 –TT Takahashi

In terms of sideslip response, the adverse yaw from the ailerons overpowers the weak static directional stability: *LCDP* = -0.003. Similarly, the weak static directional stability allows the equilibrium sideslip angle with full aileron and fixed rudder to grow quite large; $\beta_{uncoordinated}$ = -12.5° adverse – an objectionable value per MIL 8785C and MIL 1797A.

Under these flight conditions, we find that the bare airframe roll time constant is unsatisfactory: τ_{ROLL} =11.25-sec; this falls below LEVEL 3.

As with the X-15, the Bell X-2's Dutch Roll mode is the source of further trouble; see TABLE 1 (overleaf). $Cn\beta dynamic$ = +0.0029; ω_{DR} ~ 0.62 rad/sec (0.01 Hz) which is rated LEVEL 2 for a Class IV aircraft in Phase B flight. The bare airframe aerodynamic damping is substandard: ζ_{DR} ~ 0.09, which is LEVEL 2 (ζ_{DR} > .02) and nowhere near the LEVEL 1 ideals ($\omega_{DR}\zeta_{DR}$ > .35). ; In order to achieve minimum LEVEL 1 damping and a reasonable roll time constant, we need to employ a yaw-rate feedback gain of at least 1°/(°/sec) and a roll-rate feedback gain of at least 0.3°/(°/sec); this will synthesize *Cnr* ~ -4 and *Clp* ~ -3 with the byproducts of increasing *Clr* to ~1.6 and *Cnp* to -0.4. These gains are unacceptably high as a yaw rate of *r* = 20 °/sec would saturate the rudder. In addition, loop closure would mean that the X-2 would exhibit substantial roll induced adverse sideslip from *Cnp*: 1° of adverse sideslip would develop per 10°/sec roll rate. As the roll rates increase, the adverse yaw grows worse as high induced sideslip can easily lead to a spin. On the bright side, the weak static directional stability permits high yaw damping gains without destabilizing the spiral mode.

TABLE 1 - Lateral Directional Gains, Frequencies, Time Constants and Damping Ratios

KYAWDAMP	KROLLDAMP	Cnr	Clp	Clr	Cnp	Troll	Tspiral	wDR	zDR
0	0	-0.16	-0.20	0.05	0.03	11.45	STABLE	0.62	0.09
0	-0.1	-0.16	-1.14	0.05	-0.12	2.01	STABLE	0.62	0.09
0	-0.2	-0.16	-2.08	0.05	-0.28	1.10	STABLE	0.62	0.09
0	-0.3	-0.16	-3.02	0.05	-0.43	0.76	STABLE	0.62	0.09
0.25	0	-1.13	-0.20	0.44	0.03	11.45	STABLE	0.62	0.16
0.25	-0.1	-1.13	-1.14	0.44	-0.12	2.01	STABLE	0.62	0.16
0.25	-0.2	-1.13	-2.08	0.44	-0.28	1.10	STABLE	0.62	0.16
0.25	-0.3	-1.13	-3.02	0.44	-0.43	0.76	STABLE	0.62	0.16
0.5	0	-2.10	-0.20	0.82	0.03	11.45	STABLE	0.62	0.23
0.5	-0.1	-2.10	-1.14	0.82	-0.12	2.01	STABLE	0.62	0.23
0.5	-0.2	-2.10	-2.08	0.82	-0.28	1.10	STABLE	0.62	0.23
0.5	-0.3	-2.10	-3.02	0.82	-0.43	0.76	STABLE	0.62	0.23
1	0	-4.03	-0.20	1.60	0.03	11.45	STABLE	0.62	0.36
1	-0.1	-4.03	-1.14	1.60	-0.12	2.01	STABLE	0.62	0.36
1	-0.2	-4.03	-2.08	1.60	-0.28	1.10	STABLE	0.62	0.36
1	-0.3	-4.03	-3.02	1.60	-0.43	0.76	STABLE	0.62	0.36

This analysis shows that the Bell X-2 had fundamentally unsatisfactory aerodynamic characteristics for flight at Mach 3.2. Even if the rudder was unlocked and active feedback controls were applied to all aerodynamic surfaces, the resulting flying qualities would remain poor.

© 2025 –TT Takahashi

VI. Results & Conclusions

This paper demonstrates the physical limitations that the designers of high-performance aircraft must address. It presents case studies for the Bell X-2, North American X-15 and Grumman F-14A which shows that very high feedback gains are required to "tame" aircraft with poor bare airframe flying qualities.

This paper also introduces simple algebraic equations to estimate the closed-loop lateral-directional cross derivatives (*Clr* and *Cnp*) from bare-airframe aerodynamic data. It also provides simple algebraic equations to estimate the unintended yaw-due-to-roll-rate; these screening metrics do not appear to have been previously identified and published in open literature.

Through the example cases, this paper demonstrates how the bare airframe damping ratio of aircraft declines as speed and altitude increase. These example cases show successful and unsuccessful active control strategies experienced by actual aircraft.

- High-speed aircraft will require active Longitudinal damping which may require unreasonable gains to achieve even on an airframe which is inherently stable with seemingly generous control power.
- Slender high-speed capable aircraft are likely to have marginal bare airframe Lateral-Directional damping, even at low speeds. They will require active Dutch Roll damping which may be implemented as a "yaw damper" or as a "roll damper."
- High gain "yaw damper" control laws may stabilize the Dutch Roll at the expense of radically destabilizing the Spiral Mode
- Low gain "roll damper" control laws may stabilize the Dutch Roll at the expense of creating an adverse yawing moment-due-to-roll-rate (*Cnp*) which may lead to aircraft departure at high roll rates.

Acknowledgements

Professor Takahashi would like to thank his AFIT sponsor Prof. Ramana V. Grandhi for the opportunity to spend the summer at the Air Force Institute of Technology. This research was supported in part by an appointment to the Department of Defense (DOD) Research Participation Program administered by the Oak Ridge Institute for Science and Education (ORISE) through an interagency agreement between the U.S. Department of Energy (DOE) and the DOD. ORISE is managed by ORAU under DOE contract number DE-SC0014664. All opinions expressed in this paper are the authors' and do not necessarily reflect the policies and views of DOD, DOE, or ORAU/ORISE.

References

[1] Boyd, T.J.M., "On Hundred Years of G.H. Bryan's Stability in Aviation," *RAeS Journal of Aeronautical History*, Paper 2011/4, 2011, pp. 97-115.
[2] Bryan, G.H., Stability in Aviation, MacMillan, London, 1911.
[3] Bryan, G.H., and Williams, W.E., "The Longitudinal Stability of Gliders," *Proc. Royal Soc. Of London*, Series A, Vol 73, 1904, pp. 100-116.
[4] Wright, O., How We Invented the Airplane, Dover, New York, 1988. ISBN: 978-0486256627
[5] Bairstow, L., Jones, B.M. and Thompson, A.W.H., "Investigation into the Stability of an Aeroplane, with an Examination into the conditions necessary in order that the symmetric and asymmetric oscillations can be considered independently," ARC R&M 77, 1913.
[6] Etkin, B. and Reid, L.D., Dynamics of Flight: Stability and Control, 3rd Edition, Wiley, New York, 1996. ISBN: 978-0471034186
[7] Yechout, T.R., Introduction to Aircraft Flight Mechanics, 2nd Edition, AIAA, Reston, Va, 2014. https://doi.org/10.2514/4.102547
[8] https://bihrle.com/william-bihrle-jr/
[9] Anon., "Stability and Control DATCOM," USAF AFFDL, 1960.
[10] Miranda, L. R., Elliot, R. D., and Baker, W. M., "A Generalized Vortex Lattice Method for Subsonic and Supersonic Flow Applications." NASA CR 2865, 1977.
[11] Takahashi, T.T., Lorenzo, W.P., Gaydusek, B.S. and Griffin, J.A., "VORLAX 2024: Further Upgrades to a Legacy Potential Flow Solver," AIAA 2025-0848, 2025.

© 2025 –TT Takahashi

[12] DaRonch, A., Vallespin, D., Ghoreyshi, M. and Badcock, K.J., "Evaluation of Dynamic Derivatives Using Computational Fluid Dynamics," *AIAA Journal*, Vol. 50, No. 2, 2012. https://doi.org/10.2514/1.J051304
[13] Granata, D., Savino, A., and Zanotti, A., "Numerical Evaluation of Aircraft Aerodynamic Static and Dynamic Stability Derivatives by a Mid-Fidelity Approach," *MDPI Aerospace*, Vol. 11, 2024. https://doi.org/10.3390/aerospace11030213
[14] Chalk, C.R., Neal, T.P, Harris, T.M., Pritchard, F.E. and Woodcock, R.J., "Background Information and User Guide for MIL-F-8785B(ASG) "Military Specification – Flying Qualities of Piloted Airplanes"," AFFDL TR 69-72, 1969.
[15] "Military Specification, Flying Qualities of Piloted Airplanes," MIL-F-8785C, Nov. 1980
[16] "Military Standard, Flying Qualities of Piloted Vehicles," MIL-STD-1797(USAF), Mar. 1987.
[17] Bihrle, W., "A Handling Qualities Theory for Precise Flight-Path Control," AFFDL TR-65-198, 1966.
[18] Takahashi, T.T., Aircraft Performance and Sizing, Volume II: Applied Aerodynamic Design, Momentum Press, New York, 2016.
[19] Takahashi, T.T., Griffin, J.A., and Grandhi, R.V., "High-Speed Aircraft Stability and Control Metrics," *MDPI Aerospace*, Vol. 12, 2025. https://doi.org/10.3390/aerospace12010012
[20] McRuer, D.T, Graham, D. and Ashkenas, I., Aircraft Dynamics and Automatic Control, Princeton University Press, Princeton, NJ, 1973.
[21] Day, R.E., "Coupling Dynamics in Aircraft Design: A Historical Perspective," NASA SP-532, NASA, 1997.
[22] Weil, J., and Day, R.E., "An Analog Study of the Relative Importance of Various Factors Affecting Roll Coupling," NACA RM H56A06, 1956.
[23] Woodcock, R.J. and Weissman, R., "The Stall/Spin Problem," AGARD CP-199, 1976.
[24] Lorenzo, W.P. and Takahashi, T.T., "Reconstructing and Reassessing Neil Armstrong's "First Man" Flight in the North American X-15," AIAA 2024-2643, 2024.
[25] Kelley, W.W. and Enevoldson, E.K., "Limited Evaluation of an F-14A Airplane Utilizing an Aileron Rudder Interconnect Control System in the Landing Configuration," NASA TM-81972, 1981.
[26] Takahashi, T.T., "Ezra Kotcher: the Father of the Bell X-1 and X-2," Royal Aeronautical Society Journal of Aeronautical History, 2024-04, pp. 73-143, Oct. 2024.
[27] O'Brien, K.P. and Takahashi, T.T., "An Investigation of the Bell X-2 and the Factors that Led to Its Fatal Accident," AIAA 2022-3203, 2022.
[28] O'Brien, K.P. and Takahashi, T.T., "Tail Sizing Strategies to Ensure Low-Risk Maneuvering High-Speed Flight," AIAA 2024-2320, 2024.

© 2025 –TT Takahashi